DOI:10.1158/1078-0432.CCR-05-0038

Clinical Cancer Research

In vivo RNA Interference–Mediated Ablation of *MDR1* P-Glycoprotein

Andrea Pichler, Noam Zelcer, Julie L. Prior, et al.

Clin Cancer Res 2005;11:4487-4494. Published online June 15, 2005.

DOI:10.1158/1078-0432.CCR-05-0038

In vivo RNA Interference–Mediated Ablation of *MDR1* P-Glycoprotein

Andrea Pichler,[1] Noam Zelcer,[3] Julie L. Prior,[1] Annemieke J. Kuil,[3] and David Piwnica-Worms[1,2]

Abstract Multidrug resistance (MDR) remains a major obstacle to successful chemotherapeutic treatment of cancer and can be caused by overexpression of P-glycoprotein, the *MDR1* gene product. To further validate a knockdown approach for circumventing MDR, we developed a P-glycoprotein inhibition strategy using short hairpin RNA interference (shRNAi) and now show efficacy and target specificity *in vivo*. Two of eight tested shRNAi constructs targeted against human *MDR1* mRNA inhibited expression of P-glycoprotein by >90%, whereas control shRNAi had no effect. Ablation of P-glycoprotein in cells stably transduced with retroviral-mediated shRNAi was documented by Western blot and functionally confirmed by increased sensitivity of *MDR1*-transfected cells toward the cytotoxic drugs vincristine, paclitaxel, and doxorubicin as well as by transport of ^{99m}Tc-Sestamibi. shRNAi-mediated down-regulation of P-glycoprotein transport activity both in cultured cells and in tumor implants in living animals could be followed by direct noninvasive bioluminescence imaging using the *Renilla* luciferase fluorophore, coelenterazine, a known P-glycoprotein transport substrate. Furthermore, after somatic gene transfer by hydrodynamic infusion of a *MDR1-Firefly luciferase* (*MDR1-FLuc*) fusion construct into mouse liver, the effect of shRNAi delivered *in vivo* on P-glycoprotein-FLuc protein levels was documented with bioluminescence imaging using D-luciferin. ShRNAi against *MDR1* reduced bioluminescence output of the P-glycoprotein-FLuc reporter 4-fold *in vivo* compared with mice treated with control or scrambled shRNAi. Targeted down-regulation of a somatically transferred P-glycoprotein-eGFP fusion reporter also was observed using fluorescence microscopy. Our results show that shRNAi effectively inhibited *MDR1* expression and function in cultured cells, tumor implants and mammalian liver, documenting the feasibility of a knockdown approach to reversing MDR *in vivo*.

In cancer, overexpression of the multidrug resistance (*MDR1*) P-glycoprotein (ABCB1) is a possible cause of chemotherapy-based treatment failure (1–3). P-glycoprotein is a 170-kDa transmembrane protein and a member of the ATP-binding cassette transporter superfamily (4). P-glycoprotein confers cross-resistance to unrelated drugs that differ widely with respect to molecular structure and target specificity, including many natural product agents (e.g., paclitaxel, vincristine, and doxorubicin) as well as new targeted anticancer agents (e.g., Gleevec; ref. 5). P-glycoprotein acts as an energy-dependent efflux transporter that efficiently enhances outward transport and/or prevents entry of compounds, thereby resulting in decreased intracellular accumulation and decreased cytotoxicity of anticancer drugs. One approach to circumvent MDR is the use of P-glycoprotein modulators or reversal agents, compounds that inhibit the transport activity of P-glycoprotein (6). Whereas newer, more selective small molecules now in clinical trials are showing promise as reversal agents, we are interested in selectively blocking expression of *MDR1* mRNA with RNA interference (RNAi).

RNAi relies on the sequence-specific interaction between small interfering RNA (siRNA) and mRNA (7–9). Degradation of long double-stranded RNA to siRNA is mediated by a double-stranded RNA–specific endonuclease known as Dicer (10). The siRNAs are incorporated into a nuclease complex known as RNA-induced silencing complex where unwinding of the duplex siRNAs takes place. The antisense strand binds in a highly sequence-specific manner to target mRNA, which is then endonucleolytically cleaved and degraded (reviewed in ref. 11). siRNAs can be either endogenously expressed or exogenously synthesized and delivered.

In this report, we use short hairpin loop RNAi expression constructs (shRNAi) to show that endogenous as well as overexpressed P-glycoprotein can be effectively abrogated and

Authors' Affiliations: [1]Molecular Imaging Center, Mallinckrodt Institute of Radiology, [2]Department of Molecular Biology and Pharmacology, Washington University School of Medicine, St. Louis, Missouri, and [3]Division of Molecular Biology and Center of Biomedical Genetics, The Netherlands Cancer Institute, Amsterdam, the Netherlands

Received 1/6/05; revised 3/24/05; accepted 3/30/05.

Grant support: Dutch Cancer Society grant NKI 2001-2474 (P. Borst supporting the work of N. Zelcer and A.J. Kuil), NIH grant P50 CA94056, and the U.S. Department of Energy grant 94ER61885 (D. Piwnica-Worms).

The costs of publication of this article were defrayed in part by the payment of page charges. This article must therefore be hereby marked *advertisement* in accordance with 18 U.S.C. Section 1734 solely to indicate this fact.

Note: Supplementary data for this article are available at Clinical Cancer Research Online (http://clincancerres.aacrjournals.org/).

N. Zelcer is currently at the Department of Pathology and Laboratory Medicine, HHMI, University of California at Los Angeles, Los Angeles 90055 CA.

Requests for reprints: David Piwnica-Worms, Molecular Imaging Center, Mallinckrodt Institute of Radiology, Washington University School of Medicine, Box 8225, 510 South Kingshighway Boulevard, St. Louis, MO 63110. Phone: 314-362-9359; Fax: 314-362-0152; E-mail: piwnica-wormsd@mir.wustl.edu.

DOI:10.1158/1078-0432.CCR-05-0038

Table 1. Description of shRNAi Constructs Targeting *MDR1*

Construct	Target nucleotides	Sense	Loop	Antisense
1	88-110	gaaaccaactgtcagtgta	ttcaagaga	tacactgacagttggtttc
2	886-908	tatttctatggtgctgct	ttcaagaga	agcagcacctatagaaata
3	1513-1535	ggaagccaatgcctatgac	ttcaagaga	gtcataggcattggcttcc
4	1780-1802	tgctgacgtcatcgctggt	ttcaagaga	accagcgatgacgtcagca
5	2161-2183	tggaggcctgcaaccagca	ttcaagaga	tgctggttgcaggcctcca
6	2477-2499	ggggctataggttccaggc	ttcaagaga	gcctggaacctatagcccc
7	2900-2922	ctcatgagctttgaggatg	ttcaagaga	catcctcaaagctcatgag
8	3448-3470	ggaggccaacatacatgcc	ttcaagaga	ggcatgtatgttggcctcc

NOTE: Eight selected shRNAi constructs are shown with detailed description of the *MDR1* target nucleotides, sense, and antisense sequences and the loop sequence. Detailed constructs information is available as supplementary information.

sensitivity to cytotoxic drugs restored. Using noninvasive bioluminescence imaging of both P-glycoprotein transport activity and P-glycoprotein protein levels, we directly show shRNAi-mediated down-regulation of P-glycoprotein in intact cells and living animals *in vivo*.

Materials and Methods

Chemicals. Native coelenterazine (Biotium, Inc., Hayward, CA) and coelenterazine cp (Molecular Probes, Eugene, OR) were dissolved in ethanol as a 4.7 mmol/L stock solution. LY335979 (Zosuquidar trihydrochloride; gift of Eli Lilly, Indianapolis, IN) and XR9576 (Tariquidar; gift of Xenova QLT, Vancouver, Bristish Columbia, Canada) were prepared as stock solutions in DMSO. All other reagents were obtained from Sigma Chemical Co. (St. Louis, MO) and dissolved in DMSO or ethanol. Final concentrations of DMSO or ethanol did not exceed 0.1%, a concentration that had no effect on the results (data not shown).

Cell lines and culture conditions. The human colon carcinoma HCT-8 and HEK293 cell lines were maintained in RPMI and DMEM, respectively, supplemented with heat-inactivated fetal bovine serum (10%), L-glutamine (1%), and penicillin/streptomycin (0.1%) in a 5% CO_2 incubator at 37°C.

Cloning of reporter constructs. To make MDR1-eGFP, *MDR1* cDNA was excised from pGEM3Zf(−)-*Xba*I-MDR1.1 with *Xba*I. The isolated cDNA fragment was further digested with *Pst*I. The resulting 3.5 and 0.6 kb fragments were cloned into pBluescript KS to yield pBlue-N-MDR1 and pBlue-C-MDR1, respectively. To replace the *MDR1* stop codon with a *Sal*I site we did a PCR reaction using Pfu DNA polymerase with oligonucleotides MDR1-Pst-Forward (AAACTGCAG-CATTGCTGAGAAC), MDR1-Sal-reverse (GCGTCGACCTGGCGC-TTTGTTCCAGC), and pBlue-C-MDR1 as template. The resulting 476-bp PCR product was digested with *Pst*I and *Sal*I and cloned into pBlue-C-modified-MDR1. The sequence of the amplified fragment was verified by sequencing both strands. The *Pst*I/*Sal*I fragment from pBlue-C-modified-MDR1 was cloned into the *Pst*I/*Sal*I sites of pBlue-N-MDR1 to yield pBlue-modified-MDR1. The complete modified *MDR1* cDNA was excised from pBlue-modified-MDR1 by digestion with *Xba*I and *Sal*I and cloned into the *Nhe*I and *Sal*I sites of pEGFP-N3 (Clontech, Palo Alto, CA) to yield pMDR1-eGFP. The construct was verified by digestion analysis.

To make pMDR1-FLuc, eGFP was deleted from pMDR1-eGFP with *Bam*HI/*Not*I and replaced with FLuc and an 11-mer polypeptide linker from pIκBα-FLuc using *Bam*HI/*Not*I.[4] The construct was verified by digestion analysis.

[4] S. Gross and D. Piwnica-Worms, Methods in Enzymology 2005, in press.

Cloning of RNA interference constructs and generation of stable RNA interference clones. Eight different shRNAi constructs that span the entire open reading frame of *MDR1* (Table 1) were constructed and cloned into the pSuper expression system (12). HEK293 cells were transiently transfected with the shRNAi constructs together with pMDR1-eGFP and screened by fluorescence-activated cell sorting analysis for reduced GFP-mediated fluorescence. The most effective constructs (constructs 1 and 7) were subcloned into the retroviral variant of the pSuper system, pRetrosuper. Upon calcium phosphate transfections of these constructs (13), viral particles were produced in the amphotrophic packaging cell line Phoenix and were used to transduce HEK293 cells that stably over-produce the MDR1-eGFP fusion protein or the HCT-8 colon carcinoma line. As a negative control, clones were transduced with empty pRetrosuper virus. Cells were selected with 2 μg/mL puromycin and 400 nmol/L GF120918 (Elacridar; gift of GlaxoSmithKline, Research Park Triangle, NC) and clones that survived selection were expanded and analyzed for expression of P-glycoprotein.

Immunoblot analysis. *MDR1* P-glycoprotein and GFP were detected in total membrane extracts (20-100 μg protein loaded as indicated) from cell lines using monoclonal antibody C219 (Signet Laboratories, Dedham, MA; ref. 14) and monoclonal antibody ab1218 (Abcam Ltd., Cambridge, United Kingdom), respectively. Total protein was determined by bicinchoninic acid assay (Pierce Biotechnology, Inc., Rockford, IL). Equal loading was confirmed by either Ponceau S staining or with anti-β-catenin antibody (BD Biosciences PharMingen, San Diego, CA).

Cytotoxicity assay. Drug sensitivity of cells was determined using growth inhibition assays under continuous long-term drug exposure. Cells were plated at a density of 1,500 cells per well in triplicate in a 96-well plate. After 24 hours, drug in varying concentrations was added to each well. Incubations were continued for an additional 72 hours. At the end of the assay, medium was removed from the plates, and plates were frozen at −80°C for at least 4 hours. Subsequently, plates were thawed and the total number of cells was determined with fluorescence by using the CyQuant cell proliferation assay kit (Molecular Probes, Leiden, the Netherlands). Fluorescence was measured with a CytoFluor 4000 fluorescence plate reader (Applied Biosystems, Norwalk, CT). The relative resistance was calculated as the ratio of half-maximal inhibitory concentration (IC_{50}) of the resistant cell line to the IC_{50} of the parental cell line.

Cellular accumulation of ^{99m}Tc-Sestamibi. Transport function and modulation of *MDR1* P-glycoprotein with LY335979 (1 μmol/L) and XR9576 (1 μmol/L) under steady-state conditions in intact cells were assayed with ^{99m}Tc-Sestamibi as described previously (15). Cell-associated tracer (n = 4 each condition) was expressed as fmol/mg protein/$(nmol/L)_o$, where cell content of Tc-Sestamibi (fmol) was normalized to mg of cell protein and extracellular concentration of tracer ($nmol/L_o$).

DOI:10.1158/1078-0432.CCR-05-0038

Luciferase lysis assays. *Renilla* and Firefly luciferase activities in cell lysates were detected according to the manufacturer's protocol (Promega, Madison, WI) as described previously (16). In brief, cell lysates (20 μL) were mixed with *Renilla* or Firefly luciferase assay reagent (100 μL). Following a 1-minute incubation, luminescence was measured from each sample in a tabletop beta counter (Beckman Coulter, Fullerton, CA). Results were normalized to total protein as determined by bicinchoninic acid assay (Pierce Biotechnology).

Bioluminescence imaging of cell lines. Cells were transiently transfected with a codon humanized vector pRLuc-N3 (BioSignal Packard, Montreal, Quebec, Canada) for *Renilla* luciferase and pGL3-control (Promega) for Firefly luciferase at a ratio of 3:2. The next day, cells were counted and used for mouse injections (4×10^6) or seeded (2×10^5 per well) into 6-well plates. The following day, to image *Renilla* luciferase, medium was changed in the 6-well plates to a colorless solution (2.7 mmol/L KCl, 139 mmol/L NaCl, 8.1 mmol/L Na_2H-$PO_4 \cdot 7H_2O$, 1.5 mmol/L KH_2PO_4, 1.8 mmol/L $CaCl_2$, 1 mmol/L $MgCl_2$, and 5.5 mmol/L D-glucose) containing a final concentration of 400 nmol/L coelenterazine. After returning to normal growth medium for 6 hours, background images were taken to confirm the absence of signal from *Renilla* luciferase. Then the plates were imaged again in colorless solution containing 150 μg/mL D-luciferin. Bioluminescence imaging was done with the *In vivo* Imaging System (IVIS; Xenogen Corp., Alameda, CA). Acquisition times were dependent on light output and are indicated in figure legends. After images of intact cells were taken, cells were lysed to perform *Renilla* and Firefly activity assays and to document levels of *MDR1* P-glycoprotein by immunoblot. Data analysis was done as described previously (17).

Bioluminescence imaging of animals. Animal care and euthanasia were approved by the Washington University Medical School Animal Studies Committee. From the same batch of cells above, 4×10^6 of each cell line per tumor site were injected s.c. into flanks of 6-week-old male NCr *nu/nu* mice (Taconic Farms, Germantown, NY) in matrigel (BD, Franklin Lakes, NJ). One day after injection, mice were anaesthetized with 2.5% isoflurane before tail vein injection of coelenterazine (1 μg/g) formulated from an ethanol stock diluted in sodium phosphate buffer (50 mmol/L). Bioluminescence imaging was done on the IVIS at 1 and 4 minutes after injection as described previously (acquisition time, 60 seconds; binning, 8; field of view, 10 cm; f/stop, 1; ref. 17). Anesthesia was maintained during imaging by nose cone delivery of 2.5% isoflurane. Following imaging, animals were sacrificed by cervical dislocation.

In vivo transfection of mouse hepatocytes was done using the hydrodynamic method as described previously (18). Briefly, different plasmids (pMDR1-FLuc, 1 μg; pRLuc-N3, 1 μg; various shRNAi constructs, 10 μg each) were combined as indicated, diluted in phosphate buffer in a volume of 1 mL per 10 g body weight and rapidly injected into tail veins of mice (FVB/N, 6-week-old males). Rapid injection of large volumes of buffer leads to right heart failure and backflushing into the inferior vena cava. Thus, high hydrostatic pressures mechanically force DNA solution into tissues such as the liver. Putatively, membrane disruption and enhanced endocytosis promote uptake of naked DNA into hepatocytes. In spite of these seemingly harsh conditions for introducing DNA constructs into hepatocytes, all animals used in our experiments recovered from the procedure well within 4 to 6 hours. Imaging of mice was done 18 hours after somatic gene transfer by injection of coelenterazine cp (1 μg/g BW, i.v.), followed 4 hours later with injection of D-luciferin (150 μg/g BW, i.p.).

Fluorescence microscopy. For fluorescence microscopy, *in vivo* transfection of mouse hepatocytes was done as described above using pMDR1-eGFP (1 μg) and shRNAi constructs (5-10 μg each). Animals were sacrificed the next day, liver specimens collected and cryosectioned (8 μm). Sections were mounted with media containing propidium iodide (Vector Laboratories, Burlingame, CA) and examined by confocal fluorescence microscopy (Zeiss LSM 5 PASCAL system, Jena, Germany), using eGFP (488 nm ex; 505 nm em) and propidium iodide (543 nm ex; 560 nm em) spectral windows.

Data analysis. Corresponding grayscale photographs and color luciferase images were superimposed and analyzed with LivingImage (Xenogen) and Igor (Wavemetrics, Lake Oswego, OR) image analysis software. Signal intensities for *Renilla* luciferase were obtained from regions of interest defined either with a grid template for cells grown in 6-well plates or manually for tumors. Using the same regions of interest, background from images obtained 6 hours after coelenterazine addition was subtracted from images taken using D-luciferin. For 6-well plates, signals for *Renilla* and Firefly luciferase were normalized to the corresponding enzyme activity in cell lysates (cpm) and total protein (mg protein). Data were expressed as normalized photon flux (*Renilla* photons/s/cpm/mg protein over Firefly photons/s/cpm/mg protein).

For tumor model mouse experiments, raw signal intensities for *Renilla* luciferase were averaged for each independent group (three experiments with three to four animals each). Data were reported as means ± SE of total flux (photons/s). Pairs were compared with the Student's *t* test (19) and values of $P \leq 0.05$ were considered significant.

For liver transfection experiments, signal from Firefly luciferase was normalized to signal from *Renilla* luciferase to correct for transfection efficiencies in mouse livers. Averaged values (five to six animals within each group) were reported as means ± SE.

Results

Testing various constructs to knock down MDR1 P-glycoprotein. Functional RNAi constructs consist of a 19-nucleotide (nt) duplex sequence, flanked by AA at the 5′ end and TT at the 3′ end. *MDR1* mRNA contains 22 sequences that fit this specification (Supplementary Tables). Eight of these sequences covering the entire open reading frame were cloned into the pSuper expression system (12), each with constant regions flanking the sense and antisense sequences separated by a 9-nt loop (Table 1). The resulting transcripts were predicted to form a short hairpin loop. The ability of these eight constructs to reduce fluorescence in HEK293 cells that stably produced a MDR1-eGFP fusion protein was initially screened by fluorescence-activated cell sorting analysis (data not shown). Two of the shRNAi constructs tested positive in this assay (constructs 1 and 7, Table 1). To verify this result, we transiently transfected these two constructs along with two constructs that were negative in the fluorescence-activated cell sorting analysis into HEK293/MDR1-eGFP cells. After 3 days, total cell lysates were prepared and subjected to immunoblot analysis (Fig. 1). Antibodies against *MDR1* P-glycoprotein (C219) or against GFP (ab1218) showed that constructs 1 and 7 were able to abolish expression of the MDR1-eGFP fusion protein in these cells by >90%. By comparison, constructs 4 and 6 had minimal or no effect, but as expected, a combination of all constructs also showed gene silencing.

Stable expression of short hairpin RNA interference constructs in HEK293/MDR1-eGFP and HCT-8 cells. Constructs 1 and 7 were subcloned into the retroviral variant of the pSuper system, pRetrosuper (12). Viral particles were produced in the amphotrophic packaging cell line Phoenix and were used to transduce HEK293/MDR1-eGFP cells, which stably overproduced the MDR1-eGFP fusion protein, or the colon carcinoma line HCT-8, which has high levels of endogenous *MDR1* P-glycoprotein (20). As a control, cells were transduced with an empty pRetrosuper virus. Stable clones of HEK293/MDR1-eGFP cells transduced with the pRetroRNAi #1 constructs (clones 1, 2, and 4) showed complete loss of MDR1-eGFP compared with control clones (clones 3, 5, and 6). Total loss of P-glycoprotein expression was shown in a long exposure (Fig. 2A, *bottom*)

DOI:10.1158/1078-0432.CCR-05-0038

when compared with a short exposure (Fig. 2A, *top*). All stable HCT-8 clones (Fig. 2B) transduced with pRetroRNAi #1 (clones 2, 5, and 6; data not shown) showed down-regulation of P-glycoprotein. Clones transduced with pRetroRNAi #7 (clone 2; data not shown) showed a more moderate (~50%) reduction of P-glycoprotein levels when compared with control clones (clones 3 and 6). Some of these clones were tested in a standard growth inhibition assay in the presence of vincristine, a known P-glycoprotein substrate. Representative results for HEK293/MDR1-eGFP (Fig. 2C) and HCT-8 (Fig. 2D) are shown and show sensitization toward the drug in clones that stably express shRNAi constructs against *MDR1* mRNA. Similar results were obtained with paclitaxel and doxorubicin (data not shown).

Short hairpin RNA interference–mediated down-regulation of P-glycoprotein transport activity: validation by imaging intact cells. Coelenterazine, the fluorogenic substrate for *Renilla* luciferase, is transported by *MDR1* P-glycoprotein, thereby enabling P-glycoprotein transport activity to be monitored in intact cells and living animals with noninvasive bioluminescence imaging (16). We used stable clones of HCT-8 shRNAi #1 (clone 5) and HCT-8 control (clone 6) to show the effect of shRNAi in intact cells. The shRNAi and control clones were transiently transfected with vectors expressing a codon-humanized *Renilla* luciferase (pRLuc-N3) and to normalize for transfection efficiency, Firefly luciferase (pGL3-control). One day after transfection, cells were counted and separated into two groups. For group 1, 2×10^5 cells were plated in a 6-well plate. For group 2, 4×10^6 cells of the same batch were injected in matrigel pseudotumors into *nu/nu* mice (see below). The next day, intact cells of the 6-well plate were imaged using an *in vivo* imaging system (17). HCT-8 control cells, transiently expressing *Renilla* luciferase (RLuc), showed low bioluminescence due to P-glycoprotein–mediated efflux transport of coelenterazine. By comparison, transiently expressing RLuc HCT-8 cells, wherein P-glycoprotein was down-regulated with shRNAi, showed high bioluminescence (Fig. 3A). In control experiments we found levels of RLuc enzyme activity in both cell lines to be comparable in cell lysates, an assay not affected by the membrane protein P-glycoprotein (data not shown). In addition, when cell lysates were normalized for transfection efficiency and total cell protein, HCT-8 control cells had a 7.5-fold reduced signal output compared with HCT-8 shRNAi cells (Fig. 3B). Western blotting confirmed that P-glycoprotein expression was abolished in HCT-8 shRNAi cells compared with HCT-8 control cells (Fig. 3C).

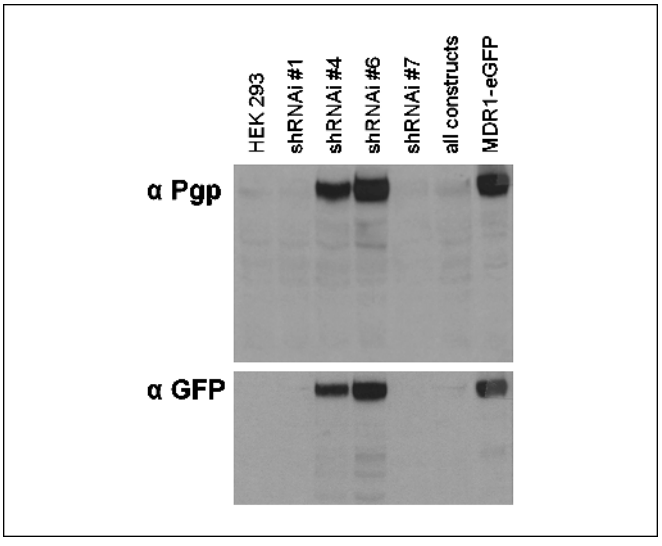

Fig. 1. Effect of transiently transfected shRNAi on expression of the fusion protein MDR1-eGFP. Expression of *MDR1* P-glycoprotein (monoclonal antibody C219) and eGFP (monoclonal antibody ab1218) were detected in total membrane extracts of parental HEK293 cells and HEK293 transiently transfected with pMDR1-eGFP in the presence of various shRNAi constructs, as labeled. Gel loading of 20 μg total protein was controlled with Ponceau S staining of blotted membranes.

To independently confirm the functional significance of P-glycoprotein levels in HCT-8 control and shRNAi cell lines, cell tracer transport assays were done with ^{99m}Tc-Sestamibi, a validated transport substrate for P-glycoprotein (21), in the absence or presence of XR9576 (1 μmol/L) and LY335979 (1 μmol/L), potent and selective modulators (inhibitors) of P-glycoprotein transport function (22, 23). ^{99m}Tc-Sestamibi accumulation in HCT-8 control cells was 4.7 fmol/mg protein/(nmol/L_o) and as expected, in HCT-8 shRNAi cells was 8- to 10-fold enhanced when compared with HCT-8 control cells, similar to the bioluminescence results. By comparison, ^{99m}Tc-Sestamibi accumulation in HCT-8 shRNAi cells also treated with XR9576 and LY335979 showed 20- and 18-fold enhancement, respectively, over HCT-8 control cells. This represented the maximum possible reversal and reflected the high sensitivity of the radiotracer assay for functionally detecting residual P-glycoprotein transport activity at levels approaching the protein detection limits of routine Western analysis. In addition, it should be noted that selection of the stable cell lines required the presence of a P-glycoprotein modulator to prevent selection for MDR; thus, nominal up-regulation of transporters cross-reacting with ^{99m}Tc-Sestamibi cannot be formally excluded.

Short hairpin RNA interference–mediated down-regulation of P-glycoprotein transport function: validation by imaging living mice. HCT-8 control and HCT-8 shRNAi cells transiently transfected with RLuc (group 2, see above) were injected 1 day after transfection in matrigel to produce pseudotumors in *nu/nu* mice. Mice were imaged the following day because the pseudotumors were transient for RLuc and would lose expression over time. The substrate (1 μg coelenterazine/g BW) was given via tail vein injection. As seen in a representative pseudocolor image of a mouse (Fig. 4A), HCT-8 control tumors showed significantly reduced *in vivo* bioluminescence compared with tumors of cells in which P-glycoprotein was down-regulated with shRNAi. The averaged total flux of all animals tested in this experiment ($n = 4$) showed that HCT-8 control tumors (4.6×10^5 photons/s) had a 6-fold reduced signal output compared with HCT-8 shRNAi tumors (29.5×10^5 photons/s; Fig. 4B). Overall, three experiments with independent transfections using three to four mice each showed similar results.

Short hairpin RNA interference–mediated down-regulation of P-glycoprotein protein levels* in vivo*: imaging somatic gene transfer. To test whether selected shRNAi expression plasmids could be delivered and down-regulate P-glycoprotein *in vivo*, a *MDR1-FLuc* target gene was first used. ShRNAi-mediated down-regulation of *MDR1* in the fusion construct should therefore result in decreased bioluminescence due to targeted down-regulation of the fusion protein. The target fusion plasmid (pMDR1-FLuc, 1 μg/mouse) was combined with a transfection control plasmid (pRLuc-N3, 1 μg/mouse) and a plasmid encoding either shRNAi against *MDR1*, scrambled

DOI:10.1158/1078-0432.CCR-05-0038

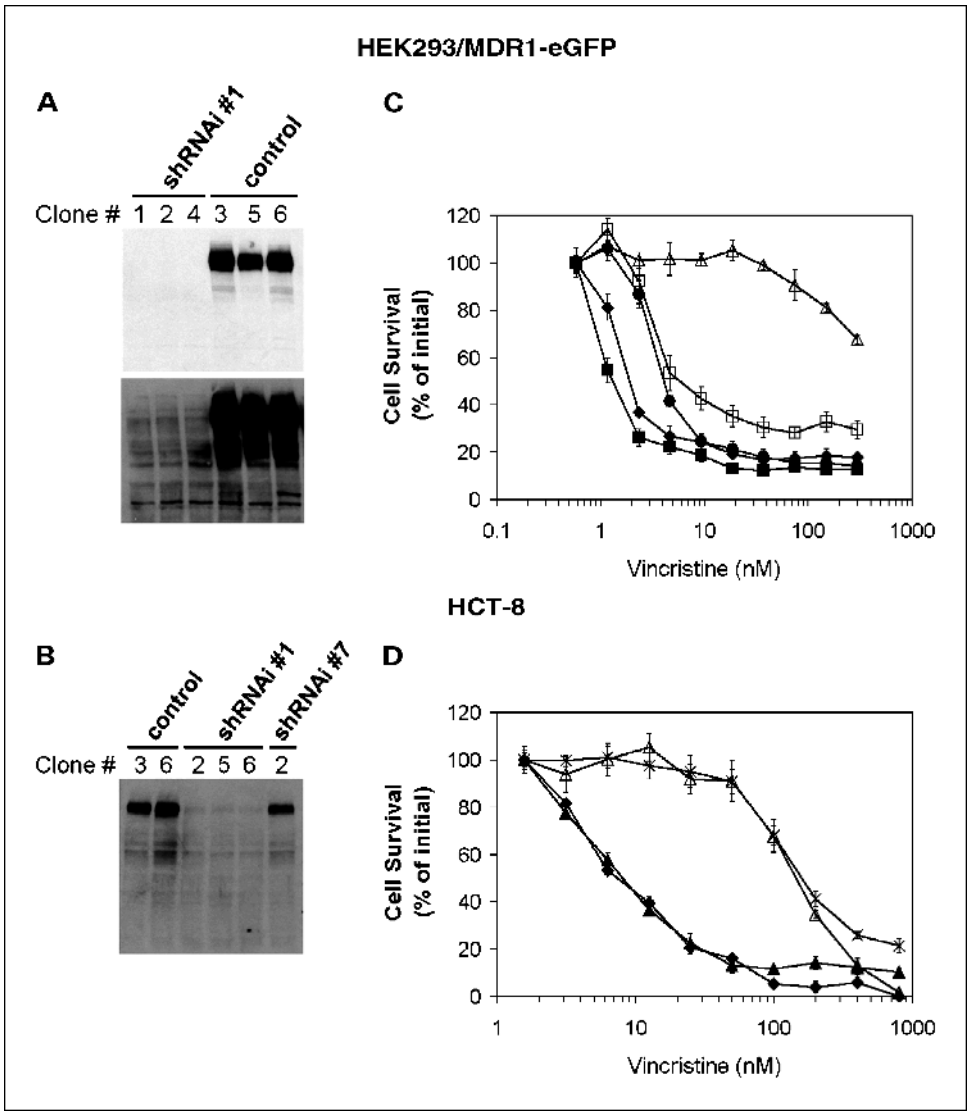

Fig. 2. Effect of stable clones of shRNAi constructs 1 and 7. *A*, expression of *MDR1* P-glycoprotein was determined in clones of HEK293/pMDR1-eGFP transduced with pRetroRNAi #1 (clones 1, 2, and 4) or transduced with an empty control vector, pRetrosuper (clones 3, 5, and 6) using monoclonal antibody C219. Short (*top*) and long (*bottom*) exposure times are shown. *B*, P-glycoprotein expression of HCT-8 clones transduced with pRetroRNAi #1 (clones 2, 5, and 6), with pRetroRNAi #7 (clone 2), and with a control virus, pRetrosuper (clones 3 and 6), were determined with monoclonal antibody C219 (20 μg total protein loaded). *C*, representative cytotoxicity assays with various concentrations of vincristine are shown for HEK293/pMDR1-eGFP control (Δ), shRNAi #1 clone 1 (♦), shRNAi #1 clone 4 (■), shRNAi #7 clone 8 (●), and for the parental cell line HEK293 (□). Percentage of growth is plotted versus vincristine concentrations (nmol/L). *D*, a similar plot for HCT-8 control clone 6 (Δ), control clone 7 (×), shRNAi #1 clone 5 (♦), and shRNAi #1 clone 10 (▲). Percentage of growth versus vincristine concentrations (nmol/L).

shRNAi or an empty vector control (10 μg/mouse). One day following somatic gene transfer by hydrodynamic transfection of mouse hepatocytes, five to six mice for each group (shRNAi, scrambled, or control) were imaged. Use of a coelenterazine derivative not transported by P-glycoprotein, coelenterazine cp (16), allowed normalization for transfection efficiencies in each mouse independent of P-glycoprotein status. Use of D-luciferin allowed documentation of the effects of various shRNAi constructs on the target fusion reporter (Fig. 5A). Scrambled or control shRNAi had no effect on P-glycoprotein-FLuc protein levels, whereas a 4-fold reduction of bioluminescence was observed when shRNAi against *MDR1* was used (Fig. 5B).

To further confirm the cellular localization and targeted down-regulation of P-glycoprotein *in vivo*, similar experiments were done with coinjection of a fluorescent fusion construct (pMDR1-eGFP, 1 μg/mouse) and plasmids encoding either shRNAi or empty vector control (5 μg/mouse). As shown in Fig. 5C, hepatocellular fluorescence was observed with a prominent perivascular pattern upon coinjection of the fusion construct and control vector, but generalized loss of hepatocellular fluorescence was observed with coinjection of the fusion and shRNAi vectors.

Discussion

A variety of novel strategies to circumvent MDR have been proposed. Among these is the use of hammerhead ribozymes against the *MDR1* mRNA (24, 25) and antisense oligonucleotides (26, 27). Both hammerhead and antisense are synthetic, must be delivered across the plasma membrane, and are susceptible to degradation. Recent studies exploiting the promise of RNAi triggered in mammalian cells (9) have led to the development of siRNAs against *MDR1* mRNA (28, 29). The data show that RNAi-triggered degradation of *MDR1* mRNA is feasible in cancer cell lines, albeit short-lived. Furthermore, Yagüe et al. (30) recently showed that the use of shRNAs, when expressed from stably integrated plasmids, can reduce *MDR1* mRNA by 95% to 97% in intact cells and restore drug sensitivity to levels equal to that of the parental cell line.

Wu et al. (29) showed that the siRNA used in their study was P-glycoprotein-specific, reversing resistance to P-glycoprotein-transported drugs whereas showing no effect on non–P-glycoprotein substrates. Maximum inhibition was only 65%, possibly due to the high basal expression levels of P-glycoprotein. In addition, the maximum decrease of *MDR1*

DOI:10.1158/1078-0432.CCR-05-0038

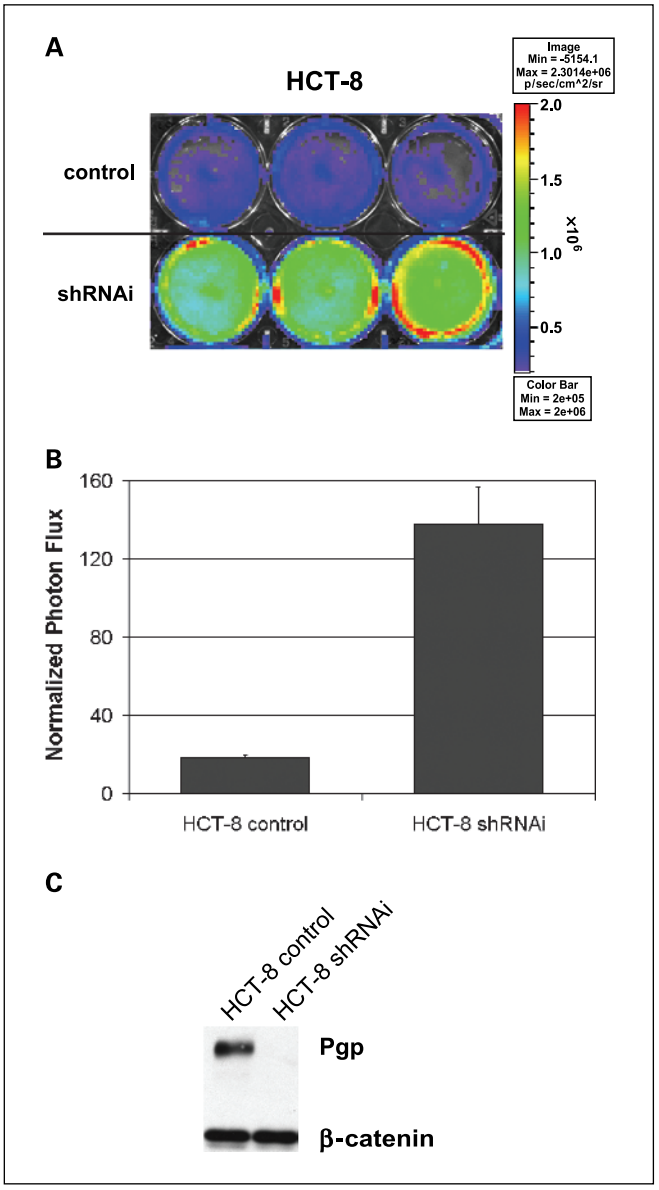

Fig. 3. Bioluminescence imaging of intact HCT-8 control and HCT-8 shRNAi cells. *A*, transiently RLuc transfected intact HCT-8 control (*top row*) and shRNAi (*bottom row*) cells were imaged in an *in vivo* imaging system upon addition of 400 nmol/L coelenterazine. Raw photon flux. *B*, quantification of data obtained from 6-well plate shown in (*A*). Total flux is corrected for *Renilla* and Firefly luciferase enzyme activity in cell lysates and normalized to total protein. *C*, expression of P-glycoprotein (*Pgp*) in the two cell lines was determined by Western blot with monoclonal antibody C219. Equal loading of 100 μg total protein was confirmed with anti-β-catenin antibody.

mRNA was only observed after 24 hours and mRNA had returned to baseline values within 72 hours. Nieth et al. (28) show that one of two tested constructs was more potent and able to reverse the MDR phenotype up to 58% in gastric cancer cells and up to 89% in pancreatic cancer cells. The more potent siRNA construct was targeted against nt 508 to 528, whereas the less effective was against nt 503 to 523, a sequence similar to that used by Wu et al. (29). The constructs most potent in our hands were targeted against nt 88 to 110 and nt 2900 to 2922 (constructs 1 and 7, respectively). Selection criteria for RNAi suggest targeting a region preferably 50 to 100 nt downstream of the start codon of the open reading frame of a given cDNA sequence (31, 32), which might explain the more potent effect of construct 1. We used constructs similar to ones described previously by Borst et al., developed to down-regulate other ABC transporters (13). Using the same vector backbone, Stege et al. (33) also describe the effectiveness of shRNAi against *MDR1* in cell culture.

In the present report, the shRNAi expression cassettes targeted against *MDR1* were used not only in cells in culture, but also in animals. Two of the eight tested constructs (constructs 1 and 7) down-regulated *MDR1* P-glycoprotein expression with construct 1 showing a more pronounced gene silencing activity than construct 7. The constructs were tested in a cell line that was constructed to overexpress a MDR1-eGFP fusion protein and in a colon carcinoma cell line with high endogenous levels of P-glycoprotein. Gene silencing induced by the pSuper and pRetrosuper constructs were specific and potent in both tested cell lines as shown with Western blotting,

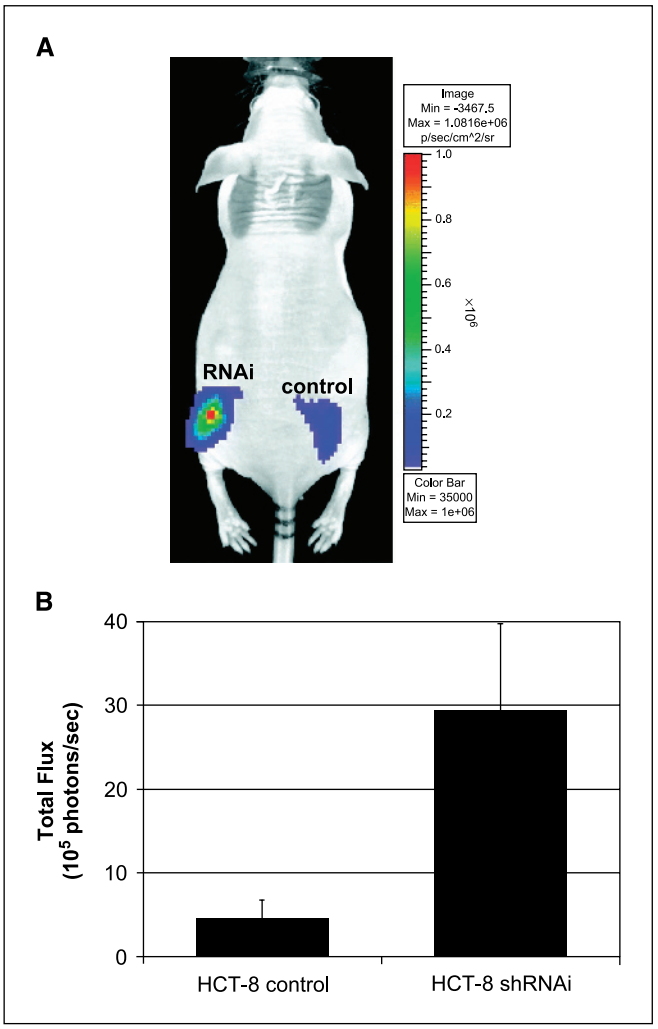

Fig. 4. Down-regulation of P-glycoprotein imaged in living mice: shRNAi-mediated reduction in outward transport function. *A*, transiently RLuc tranfected HCT-8 control and HCT-8 shRNAi cells (4×10^6 each) were injected with matrigel into *nu/nu* mice as indicated. Representative pseudocolor image 4 minutes after tail vein injection of 1 μg/g coelenterazine. *B*, total flux (photons/s) of *Renilla* luciferase signals were averaged for a representative group of animals ($n = 4$). Columns, means; bars, ±SE ($P < 0.035$).

DOI:10.1158/1078-0432.CCR-05-0038

cytotoxicity assays, radiotracer assays, and bioluminescence. In addition, the effect of P-glycoprotein silencing in cell lines that stably express shRNAi persisted for several months without selection, a result in contrast to the short-lived effects of previous siRNA strategies.

The treatment of P-glycoprotein-expressing cells with shRNAi against *MDR1* mRNA significantly enhanced the cytotoxicity of vincristine (Fig. 2C and D), paclitaxel and doxorubicin (data not shown). Furthermore, P-glycoprotein-mediated transport activity was monitored noninvasively with RLuc and bioluminescence (16). Using this technique, we could directly monitor functional down-regulation of human *MDR1* in cells and living mice. Indeed, data showed that HCT-8 cells with shRNAi against *MDR1* mRNA produced ~8-fold increased light output compared with control cells as a result of reduced outward transport of coelenterazine, the RLuc substrate. The same effect was also detected *in vivo* in mice with RLuc-expressing tumors of HCT-8 control and HCT-8 shRNAi cells.

Importantly, using a *MDR1-FLuc* fusion construct, *in vivo* down-regulation of P-glycoprotein protein levels could be directly and noninvasively visualized in living animals, following injection of D-luciferin, the FLuc substrate. *In vivo* delivery of shRNAi targeting *MDR1-FLuc* stably expressed in mouse livers showed a specific 4-fold reduction in FLuc-mediated bioluminescence. Scrambled shRNAi sequences or an empty vector plasmid had no effect on light output. Similar experiments were done with hydrodynamic liver injections of pMDR1-eGFP combined with the same shRNAi constructs. Using fluorescence microscopy of liver sections, down-regulation of the MDR1-eGFP fusion was only detected in mice treated with shRNAi against *MDR1* and not in control mice. Thus, targeted delivery and functional expression of shRNAi is feasible *in vivo* and can be used to down-regulate expression of *MDR1* mRNA.

Hydrodynamic liver injections result in transfection of mainly hepatocytes as described previously (18) and confirmed herein with the MDR1-eGFP fusion construct. Although the shRNAi and fusion reporter constructs were injected simultaneously into mice, they were not located on the same plasmid or precomplexed as done with tissue culture transfection reagents. Thus, 10-fold excess of shRNAi over the reporter construct was used to enhance the probability that both constructs targeted the same cell. Furthermore, when we used only 5-fold excess shRNAi, we still observed down-regulation of MDR1-eGFP (Fig. 5C).

Several Food and Drug Administration–approved single photon emission computed tomography radiopharmaceuticals, such as ^{99m}Tc-Sestamibi and ^{99m}Tc-Tetrofosmin, exist for clinical imaging of *MDR1* P-glycoprotein activity (5, 6, 34–38) and have the potential to monitor the effects of *MDR1*-targeted shRNAi in patients and clinical trials. However, radionuclide-based imaging with micro–single photon emission computed tomography in mice before and after treatment with *MDR1*-specific shRNAi was not feasible in this study because the selected RNAi constructs were targeted against human, not mouse, *MDR1*. Furthermore, the overall low percentage of liver cell transduction with the hydrodynamic transfection method would not be sufficient to enable differentiation between background mouse P-glycoprotein and a subpopulation of human *MDR1* P-glycoprotein in untreated versus shRNAi

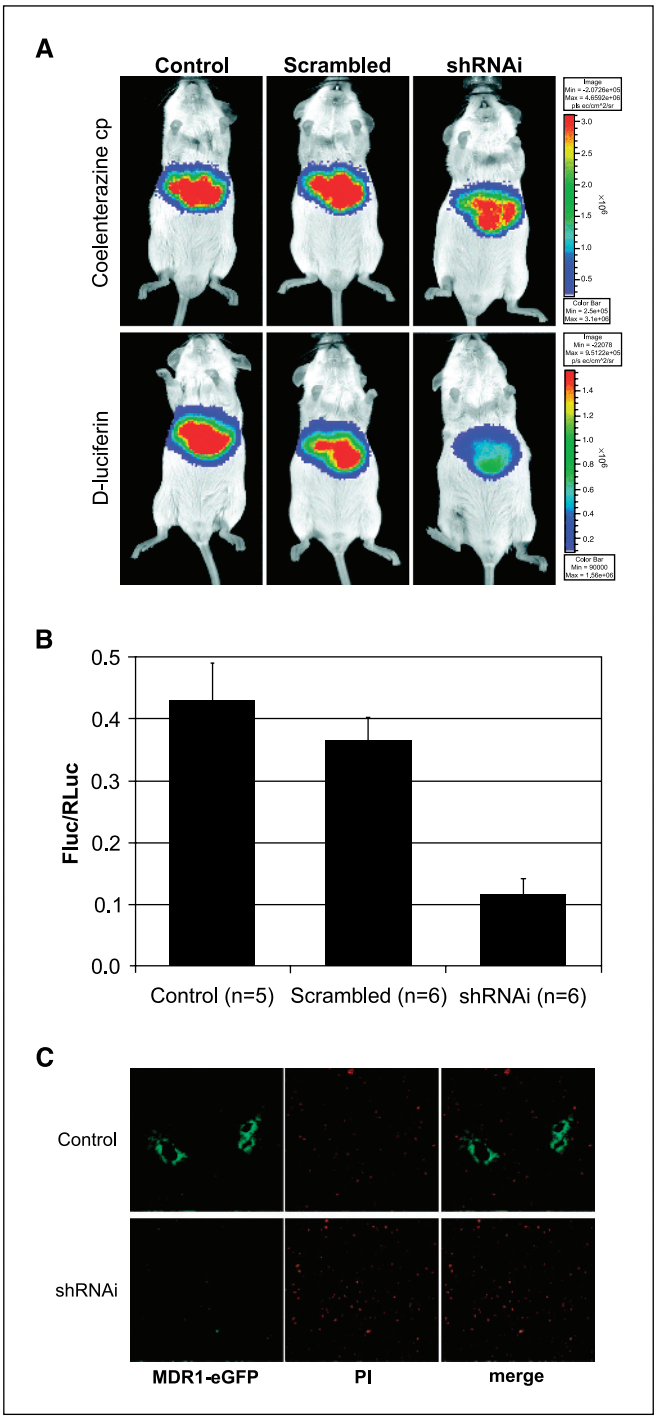

Fig. 5. Down-regulation of P-glycoprotein *in vivo*: shRNAi-mediated reduction in P-glycoprotein protein levels. *A*, representative bioluminescence images of RLuc expression with coelenterazine cp (*top*) and P-glycoprotein-FLuc expression with D-luciferin (*bottom*). Mice were hydrodynamically transfected with pMDR1-FLuc (1 μg) combined with pRLuc-N3 (1 μg; as transfection control) and treated as indicated with 10-fold excess of control (*left*), scrambled shRNAi (*middle*), or shRNAi against *MDR1* (*right*). *B*, quantification of data obtained from animals treated with control ($n = 5$), scrambled shRNAi ($n = 6$), or shRNAi against *MDR1* ($n = 6$). Columns, total flux ratio of FLuc/RLuc to correct for variation in injections of expression cassettes; bars, ±SE. $P < 0.002$ comparing control mice with shRNAi treated mice; $P < 0.003$ comparing scrambled treated mice with shRNAi treated mice. *C*, fluorescence confocal microscopy images (10×) from liver cryosections harvested from animals hydrodynamically transfected with pMDR1-eGFP (1 μg) and 5-fold excess of control (*top*) or shRNAi (*bottom*). Tissue fluorescence emitted by excitation of eGFP (*left*), by excitation of propidium iodide (*middle*), and merged images (*right*).

DOI:10.1158/1078-0432.CCR-05-0038

treated livers by ^{99m}Tc-Sestamibi imaging of the liver. It was for lack of background activity that we showed proof-of-principle shRNAi therapeutics *in vivo* with the bioluminescent targets RLuc and P-glycoprotein-FLuc in mice, but ^{99m}Tc-Sestamibi imaging may be useful for monitoring MDR therapy in clinical studies with patients.

The potent and ubiquitous gene-silencing mechanism of RNAi is generating considerable excitement in the fields of molecular biology and gene therapy (39), but delivery is probably the single biggest obstacle to the development of RNAi-based therapeutic agents (11). For clinical application, complexities in the use of shRNAi against P-glycoprotein may arise from physiologic expression of *MDR1* in several epithelial and endothelial cells (e.g., expression of P-glycoprotein in the blood-brain barrier), wherein an important role of this transporter is evident in prevention of neurotoxicity (40, 41). Therefore, it will be important to restrict delivery of RNAi to P-glycoprotein-expressing cancer cells. Use of antigen-modified retroviral- and adenoviral-based as well as other vector systems may minimize problems associated with targeted delivery of siRNAs. Indeed, a recent report describes an adenoviral vector targeted to MDR cancer cells (42), which may provide a novel strategy for combination therapeutic specificity.

In summary, our study showed enhanced effectiveness of retroviral-mediated shRNAi targeted against *MDR1* mRNA. Imaging P-glycoprotein transport activity and inhibition in a variety of tissues within the intact animal and direct documentation of shRNAi-targeted effects *in vivo* using bioluminescence provide further evidence to establish the potential of knockdown strategies for circumventing multidrug resistance.

Acknowledgments

We thank P. Borst for comments on the article and T.R. Brummelkamp, R. Benards, and R. Agami (The Netherlands Cancer Institute) for their advice and help in shRNAi vector construction.

References

1. Ling V. Multidrug resistance and P-glycoprotein expression. Ann N Y Acad Sci 1987;507:7–8.
2. Bradley G, Ling V. P-glycoprotein, multidrug resistance and tumor progression. Cancer Metastasis Rev 1994;13:223–33.
3. Borst P, Elferink RO. Mammalian ABC transporters in health and disease. Annu Rev Biochem 2002;71:537–92.
4. Dean M, Rzhetsky A, Allikmets R. The human ATP-binding cassette (ABC) transporter superfamily. Genome Res 2001;11:1156–66.
5. Gottesman M, Fojo T, Bates S. Multidrug resistance in cancer: role of ATP-dependent transporters. Nat Rev Cancer 2002;2:48–58.
6. Bates SF, Chen C, Robey R, Kang M, Figg WD, Fojo T. Reversal of multidrug resistance: lessons from clinical oncology. Novartis Found Symp 2002;243:83–96; discussion 96–102, 180–5.
7. Caplen NJ, Mousses S. Short interfering RNA (siRNA)-mediated RNA interference (RNAi) in human cells. Ann N Y Acad Sci 2003;1002:56–62.
8. Agrawal N, Dasaradhi PV, Mohmmed A, Malhotra P, Bhatnagar RK, Mukherjee SK. RNA interference: biology, mechanism, and applications. Microbiol Mol Biol Rev 2003;67:657–85.
9. Elbashir SM, Harborth J, Lendeckel W, Yalcin A, Weber K, Tuschl T. Duplexes of 21-nucleotide RNAs mediate RNA interference in cultured mammalian cells. Nature 2001;411:494–8.
10. Bernstein E, Caudy AA, Hammond SM, Hannon GJ. Role for a bidentate ribonuclease in the initiation step of RNA interference. Nature 2001;409:363–6.
11. Stevenson M. Therapeutic potential of RNA interference. N Engl J Med 2004;351:1772–7.
12. Brummelkamp TR, Bernards R, Agami R. A system for stable expression of short interfering RNAs in mammalian cells. Science 2002;296:550–3.
13. Reid G, Wielinga P, Zelcer N, et al. The human multidrug resistance protein MRP4 functions as a prostaglandin efflux transporter and is inhibited by nonsteroidal antiinflammatory drugs. Proc Natl Acad Sci U S A 2003;100:9244–9.
14. Rao V, Dahlheimer J, Bardgett M, et al. Choroid plexus epithelial expression of MDR1 P-glycoprotein and multidrug resistance-associated protein contribute to the blood-cerebrospinal fluid drug-permeability barrier. Proc Natl Acad Sci U S A 1999;96:3900–5.
15. Piwnica-Worms D, Rao V, Kronauge J, Croop J. Characterization of multidrug-resistance P-glycoprotein transport function with an organotechnetium cation. Biochemistry 1995;34:12210–20.
16. Pichler A, Prior J, Piwnica-Worms D. Imaging reversal of multidrug resistance in living mice with bioluminescence: *MDR1* P-glycoprotein transports coelenterazine. Proc Natl Acad Sci U S A 2004;101:1702–7.
17. Luker G, Bardill J, Prior J, Pica C, Piwnica-Worms D, Leib D. Noninvasive bioluminescence imaging of herpes simplex virus type 1 infection and therapy in living mice. J Virol 2002;76:12149–61.
18. Liu F, Song Y, Liu D. Hydrodynamics-based transfection in animals by systemic administration of plasmid DNA. Gene Ther 1999;6:1258–66.
19. Glantz SA. Primer of biostatistics. 2nd ed. New York: Mcgraw-Hill, Inc.; 1987. p. 379.
20. Kool M, de Haas M, Scheffer GL, et al. Analysis of expression of cMOAT (MRP2), MRP3, MRP4, and MRP5, homologues of the multidrug resistance-associated protein gene (MRP1), in human cancer cell lines. Cancer Res 1997;57:3537–47.
21. Piwnica-Worms D, Chiu M, Budding M, Kronauge J, Kramer R, Croop J. Functional imaging of multidrug-resistant P-glycoprotein with an organotechnetium complex. Cancer Res 1993;53:977–84.
22. Mistry P, Stewart A, Dangerfield W, et al. *In vitro* and *in vivo* reversal of P-glycoprotein-mediated multidrug resistance by a novel potent modulator, XR9576. Cancer Res 2001;61:749–58.
23. Dantzig A, Shepard R, Cao J, et al. Reversal of P-glycoprotein-mediated multidrug resistance by a potent cyclopropyldibenzosuberane modulator, LY335979. Cancer Res 1996;56:4171–9.
24. Kobayashi H, Dorai T, Holland JF, Ohnuma T. Reversal of drug sensitivity in multidrug-resistant tumor cells by an MDR1 (PGY1) ribozyme. Cancer Res 1994;54:1271–5.
25. Holm PS, Scanlon KJ, Dietel M. Reversion of multidrug resistance in the P-glycoprotein-positive human pancreatic cell line (EPP85-181RDB) by introduction of a hammerhead ribozyme. Br J Cancer 1994;70:239–43.
26. Liu C, Qureshi IA, Ding X, et al. Modulation of multidrug resistance gene (mdr-1) with antisense oligodeoxynucleotides. Clin Sci (Lond) 1996;91:93–8.
27. Stuart DD, Kao GY, Allen TM. A novel, long-circulating, and functional liposomal formulation of antisense oligodeoxynucleotides targeted against MDR1. Cancer Gene Ther 2000;7:466–75.
28. Nieth C, Priebsch A, Stege A, Lage H. Modulation of the classical multidrug resistance (MDR) phenotype by RNA interference (RNAi). FEBS Lett 2003;545:144–50.
29. Wu H, Hait WN, Yang JM. Small interfering RNA-induced suppression of MDR1 (P-glycoprotein) restores sensitivity to multidrug-resistant cancer cells. Cancer Res 2003;63:1515–9.
30. Yague E, Higgins CF, Raguz S. Complete reversal of multidrug resistance by stable expression of small interfering RNAs targeting MDR1. Gene Ther 2004;11:1170–4.
31. Elbashir SM, Harborth J, Weber K, Tuschl T. Analysis of gene function in somatic mammalian cells using small interfering RNAs. Methods 2002;26:199–213.
32. Reynolds A, Leake D, Boese Q, Scaringe S, Marshall WS, Khvorova A. Rational siRNA design for RNA interference. Nat Biotechnol 2004;22:326–30.
33. Stege A, Priebsch A, Nieth C, Lage H. Stable and complete overcoming of MDR1/P-glycoprotein-mediated multidrug resistance in human gastric carcinoma cells by RNA interference. Cancer Gene Ther 2004;11:699–706.
34. Ciarmiello A, Del Vecchio S, Silvestro P, et al. Tumor clearance of technetium-99m-Sestamibi as a predictor of response to neoadjuvant chemotherapy for locally advanced breast cancer. J Clin Oncol 1998;16:1677–83.
35. Sharma V, Piwnica-Worms D. Monitoring multidrug resistance P-glycoprotein drug transport activity with single-photon emission computed tomography and positron emission tomography radiopharmaceuticals. Top Curr Chem 2005;252:155–78.
36. Sukan A, Yapar Z, B SA, et al. 99mTc tetrofosmin scintigraphy in acute leukaemia: the relationship between marrow uptake of tetrofosmin and P-glycoprotein and chemotherapy response. Nucl Med Commun 2004;25:777–85.
37. Chen C, Meadows B, Regis J, et al. Detection of *in vivo* P-glycoprotein inhibition by PSC 833 using Tc-99m-Sestamibi. Clin Cancer Res 1997;3:545–52.
38. Kao C-H, Hsieh J-F, Tsai S-C, Ho Y-J, Chang Lai S-P, Lee J-K. Paclitaxel-based chemotherapy for non-small cell lung cancer: predicting the response with ^{99m}Tc-Tetrofosim chest imaging. J Nucl Med 2001;42:17–20.
39. Shankar P, Manjunath N, Lieberman J. The prospect of silencing disease using RNA interference. J Am Med Assoc 2005;293:1367–73.
40. Begley DJ. ABC transporters and the blood-brain barrier. Curr Pharm Des 2004;10:1295–312.
41. Schinkel A, Smit J, van Tellingen O, et al. Disruption of the mouse *mdr1a* P-glycoprotein gene leads to a deficiency in the blood-brain barrier and to increased sensitivity to drugs. Cell 1994;77:491–502.
42. Holm PS, Lage H, Bergmann S, et al. Multidrug-resistant cancer cells facilitate E1-independent adenoviral replication: impact for cancer gene therapy. Cancer Res 2004;64:322–8.